Int. J. Heat Mass Transfer. Vol. 30, No. 11, pp. 2271–2279, 1987
Printed in Great Britain

0017-9310/87 $3.00 + 0.00

Surface renewal theory for turbulent mixed convection in vertical ducts

LARRY W. SWANSON and IVAN CATTON
Mechanical, Aerospace and Nuclear Engineering Department, University of California, Los Angeles, Los Angeles, CA 90024, U.S.A.

(*Received* 3 *November* 1986 *and in final form* 26 *March* 1987)

Abstract—A heat transfer correlation for opposing mixed turbulent convection in vertical ducts was obtained utilizing surface renewal theory. The correlation was found to be

$$Nu_{D_h} = 0.0115 Re_{D_h}^{0.8} Pr^{0.5} \left\{1 + \left[1 - \frac{696}{Re_{D_h}^{0.8}} + 8300 \frac{Gr_{D_h}}{Re_{D_h}^{2.6}(Pr^{0.5}+1)}\right]^{0.39}\right\}.$$

The correlation fit data to within 7% over a parameter range of $0.7 < Pr < 7$, $1 \times 10^4 < Re_{D_h} < 2 \times 10^4$, and $1 \times 10^6 < Gr_{D_h} < 2 \times 10^9$. The mean residence time, characterizing the time a clump of fluid resides on the wall, was found to decrease as both $Gr_{D_h}/Re_{D_h}^{2.6}(Pr^{0.5}+1)$ and Re_{D_h} increase. This explains the enhanced heat transfer due to buoyancy in opposing mixed turbulent flows. This heat transfer enhancement was also reflected in a decreasing thermal boundary layer thickness with increasing Re_{D_h}, Gr_{D_h} or Pr.

INTRODUCTION

COMBINED turbulent convection refers to fluid flow influenced by both buoyancy forces and dynamic pressure forces. The buoyancy forces can act in either the same (aiding) or opposite direction (opposing) to the dynamic pressure forces. In heated vertical ducts with equal wall temperatures or equal wall heat fluxes symmetry can be imposed and the duct half width becomes the characteristic dimension. The density gradient across the duct half width, due to the difference in the wall and free stream temperatures, drives the buoyant layer upward near the hot wall. This layer entrains fluid from the downward flowing free stream. The net mass flow through the duct, which remains constant, determines the magnitude of the forced flow. The main concern in these flow systems lies in how these opposing forces influence flow structure and heat transfer.

Studies of mixed turbulent flows conducted over the past 50 years have dealt with either air or water flowing in horizontal or vertical ducts and tubes. Nakajima *et al.* [1] examined turbulent mixed convection between parallel vertical plates for air both experimentally and theoretically. Both aiding and opposing buoyancy flows were treated for fully developed flow with $Gr/Re^2 < 2 \times 10^{-2}$. Results showed that the Nusselt number increased with increasing Gr/Re^2 (based on duct width) for forced flow with an opposing buoyancy force, and decreased with increasing Gr/Re^2 for forced flow with an aiding buoyancy force. This phenomenon was attributed to an increasing velocity fluctuation (eddy size) in opposing flow and vice versa for aiding flow. Theoretically, Nakajima *et al.* derived a modified Van Driest damping factor which incorporated a buoyancy force in a non-isothermal field for fully developed flow. This damping factor was used in conjunction with the forced convection 'mixing length' theory of Cebeci [2] to model turbulence via an eddy diffusivity. Nakajima *et al.* noted that the model contained a shortcoming found in most eddy diffusivity models; namely, that turbulent diffusion goes to zero at a maximum or minimum point in the velocity field. In many cases combined turbulent flow fields display both maximum and minimum flow velocities where turbulent diffusion cannot be neglected. Doshi and Gill [3] have developed an improved mixing length theory which alleviates this shortcoming for purely forced convection. Even though Nakajima *et al.*'s model incorporates buoyancy effects into the damping factor, it seems that these forces should also be included in the actual 'mixing length' theory as proposed by Oosthuizen [4] for vertical plates. Despite these arguments, the theoretical predictions of heat transfer and the distribution of eddy diffusivity showed good agreement with experimental data.

Jackson and Fewster [5] studied turbulent mixed convection for water flowing in vertical tubes both experimentally and theoretically. A similar theoretical approach for the same geometry has been presented in Axcell and Hall [6] for air and Jackson [7] for liquid metals. Jackson's method combined the buoyancy force with the shear stress by evaluating the change in shear stress across the buoyant layer given by the integral

$$\Delta\sigma_{\delta_b} = \int_0^{\delta_b} (\rho_b - \rho) g \, dy.$$

Adding the change in shear stress across the buoyant

NOMENCLATURE

C_f	coefficient of friction
D	duct half width
D_h	hydraulic diameter ($4D$)
g	gravitational constant
Gr_{D_h}	Grashof number, $g\beta(T_w^*-T_e^*)D_h^3/\nu^2$
Nu_{D_h}	Nusselt number, $q_w D_h/k(T_w^*-T_e^*)$
P	pressure, $P^*/\rho u_{ave}^2$
Pe_{D_h}	Peclet number, $Pr\,Re_{D_h}$
Pr	Prandtl number, ν/α
q	heat flux
Re_{D_h}	Reynolds number, $u_{ave}D_h/\nu$
t	time, t^*u_{ave}/D_h
T	temperature, $(T^*-T_e^*)/(T_w^*-T_e^*)$
u	x-directed velocity, u^*/u_{ave}
x	vertical spatial coordinate parallel to the duct walls, x^*/D_h
y	spatial coordinate perpendicular to the duct walls, y^*/D_h.

Greek symbols

α	thermal diffusivity
β	thermal expansion coefficient
δ	buoyant layer thickness
ν	kinematic viscosity
ρ	density
σ	shear stress, $\sigma^*/\rho u_{ave}^2$
τ	mean walk residence time, $\tau^* u_{ave}/D_h$.

Subscripts

ave	average
b	bulk
D_h	hydraulic diameter
e	free stream
w	wall
0	value for pure force convection.

Superscripts

*	dimensional quantity.

layer to the shear stress at the wall yielded a modified shear stress which was used to modify the forced convection heat transfer correlation ($Nu_{D_h,0}$) of Petukhov and Kirillov [8]. By proper parameter adjustment, the correlation was made to fit data over a wide mixed flow parameter range. The correlation was found to be

$$\frac{Nu_{D_h}}{Nu_{D_h,0}} = (1+4500\overline{Gr}_{D_h}\,Re_{D_h}^{-21/8}\,Pr^{-1/2})^{0.31} \tag{1}$$

where

$$Nu_{D_h,0} = \frac{Re_{D_h}\,Pr\dfrac{C_f}{2}}{12.7\left(\dfrac{C_f}{2}\right)^{1/2}(Pr^{2/3}-1)+1.07}$$

$$C_f = \frac{1}{(3.64\log_{10}Re_{D_h}-3.28)^2} \tag{2}$$

$$\overline{Gr}_{D_h} = \frac{(\rho_b-\bar{\rho})gD_h^3}{\rho_b\nu^3}$$

and

$$\bar{\rho} = \frac{1}{T_w-T_b}\int_{T_w}^{T_b}\rho\,dT. \tag{3}$$

The above relationship agrees very well with data for water flowing in vertical pipes over the range $10^{-5} < \overline{Gr}_{D_h}/(Re_{D_h}^{21/8}\,Pr^{1/2}) < 0.2$. The correlation moderately overpredicts the data of Watzinger and Johnson [9] and Herbert and Sterns [10].

The literature discussed to this point has dealt with either duct or pipe geometries of various vertical aspect ratios covering a fairly wide range of flow parameters. In this work, surface renewal theory has been used to obtain a heat transfer correlation for opposing mixed turbulent convection in vertical ducts. The correlation applies to air, water and Freon 113 spanning a parameter range of $0.7 < Pr < 7$, $1\times10^4 < Re_{D_h} < 2\times10^4$, and $1\times10^6 < Gr_{D_h} < 1\times10^9$.

SURFACE RENEWAL THEORY

In recent years, surface renewal theory has been used successfully by Thomas and co-workers [11–15] to model fluid flow and heat transfer phenomena for a variety of flow systems. Originally, the theory was proposed by Higbie [16], Danckwerts [17] and Einstein and Li [18]. The surface renewal concept focuses on replenishing fluid in the thin layer near a heated wall. The flow mechanism is depicted in Fig. 1. A clump of fluid enters the wall layer and impinges on the wall where it remains stationary for a while. After absorbing energy, the clump then bursts off the wall and passes through the layer returning to the free stream. Since most of the thermal resistance occurs near the wall, an accurate description of the heat transfer phenomena in this layer should produce a good heat transfer correlation. The following conditions are assumed to hold inside the wall layer:

(1) constant fluid properties;
(2) incompressible flow;
(3) hydrodynamically and thermally fully developed flow;
(4) boundary layer approximation;
(5) Boussinesq approximation;
(6) x-directed convective term in the energy equation is small.

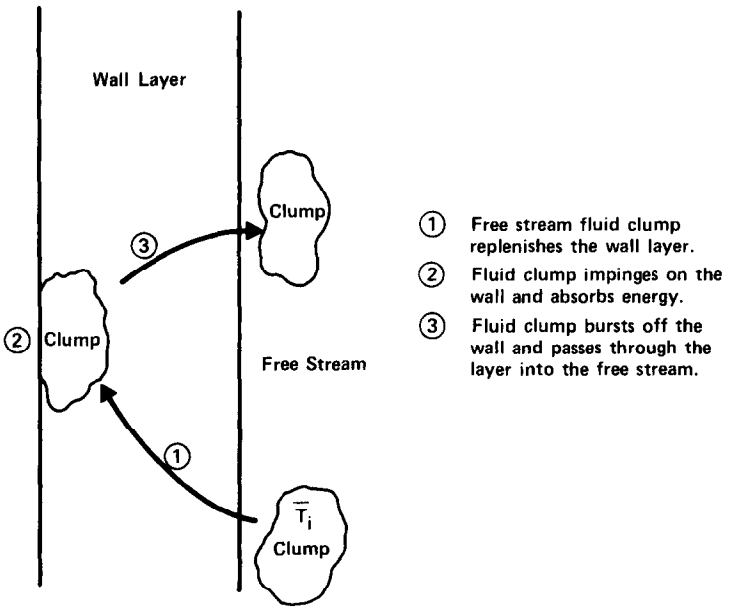

FIG. 1. Surface renewal flow mechanism.

Conditions 3, 4 and 6 have been imposed based on experimental observations found in ref. [21]. Utilizing the above assumptions, the unsteady behavior of a clump of fluid for two-dimensional parallel flow near a wall can be described by

$$\frac{\partial u}{\partial t} = -\frac{\partial P}{\partial x} - \frac{Gr_{D_h}}{Re_{D_h}^2}T + \frac{1}{Re_{D_h}}\frac{\partial^2 u}{\partial y^2} \tag{4a}$$

$$\frac{\partial T}{\partial t} = \frac{1}{Pe_{D_h}}\frac{\partial^2 T}{\partial y^2} \tag{4b}$$

with the following initial and boundary conditions

$$t = 0; \quad u = u_i, \quad T = T_i$$

$$y = 0; \quad u = 0, \quad \frac{\partial T}{\partial y} = -Nu_{D_h}$$

$$y \to \infty; \quad \frac{\partial u}{\partial y} = \frac{\partial T}{\partial y} = 0.$$

Note that the boundary condition at $y = 0$ imposes a constant wall heat flux. Time averaged variables are defined as

$$\bar{u} = \int_0^\infty u(t, y)\phi(t)\,\mathrm{d}t$$

$$\bar{P} = \int_0^\infty P(t, x)\phi(t)\,\mathrm{d}t$$

$$\bar{T} = \int_0^\infty T(t, y)\phi(t)\,\mathrm{d}t$$

where $\phi(t)$ is the contact time distribution function which represents the fraction of eddies with a wall contact time between t and $t+\mathrm{d}t$. Thomas has found that Danckwerts' random contact time distribution [17] yields good results for turbulent flows, namely

$$\phi(t) = \frac{1}{\tau}e^{-t/\tau}$$

where τ is the dimensionless mean wall residence time. Multiplying equation set (4) by $\phi(t)$ and integrating with respect to time from 0 to ∞ gives

$$\frac{1}{\tau}\bar{u} - \frac{1}{\tau}\bar{u}_i = -\frac{\mathrm{d}\bar{P}}{\mathrm{d}x} - \frac{Gr_{D_h}}{Re_{D_h}^2}\bar{T} + \frac{1}{Re_{D_h}}\frac{\mathrm{d}^2\bar{u}}{\mathrm{d}y^2} \tag{5a}$$

$$\frac{1}{\tau}\bar{T} - \frac{1}{\tau}\bar{T}_i = \frac{1}{Pe_{D_h}}\frac{\mathrm{d}^2\bar{T}}{\mathrm{d}y^2} \tag{5b}$$

with boundary conditions

$$y = 0; \quad \bar{u} = 0, \quad \frac{\mathrm{d}\bar{T}}{\mathrm{d}y} = -Nu_{D_h}$$

$$y \to \infty; \quad \frac{\mathrm{d}\bar{u}}{\mathrm{d}y} = \frac{\mathrm{d}\bar{T}}{\mathrm{d}y} = 0.$$

The energy equation is independent of the momentum equation and can be solved by inspection giving

$$\bar{T} = \bar{T}_i + \frac{Nu_{D_h}}{b}e^{-by} \tag{6}$$

where

$$b = \sqrt{\left(\frac{Pr\,Re_{D_h}}{\tau}\right)}.$$

This result is then substituted into equation (5a) which is then solved by use of integrating factors giving

$$\bar{u} = \left(\bar{u}_i - \tau\frac{\mathrm{d}\bar{P}}{\mathrm{d}x} - \tau\frac{Gr_{D_h}}{Re_{D_h}^2}\bar{T}_i\right)(1 - e^{-ay}) - \frac{Gr_{D_h}\,Nu_{D_h}\,\tau^{3/2}}{Pr^{1/2}(Pr-1)Re_{D_h}^{5/2}}(e^{-ay} - e^{-by}) \tag{7}$$

where

$$a = \sqrt{\left(\frac{Re_{D_h}}{\tau}\right)}.$$

At $y = 0$, $\bar{T} = 1$, and equation (6) becomes

$$Nu_{D_h} = b(1-\bar{T}_i) = \frac{Pr^{1/2}\, Re_{D_h}^{1/2}}{\tau^{1/2}}(1-\bar{T}_i). \quad (8)$$

Substituting this expression into equation (7) gives

$$\bar{u} = \left(\bar{u}_i - \tau\frac{d\bar{P}}{dx} - \tau\frac{Gr_{D_h}}{Re_{D_h}^2}\bar{T}_i\right)(1-e^{-ay}) - \frac{Gr_{D_h}(1-\bar{T}_i)\tau}{(Pr-1)Re_{D_h}^2}(e^{-ay}-e^{-by}). \quad (9)$$

The dimensionless wall shear stress is defined as

$$\sigma_0 = \frac{d\bar{u}}{dy} = \frac{Re_{D_h}^{1/2}\bar{u}_i}{\tau^{1/2}} - Re_{D_h}^{1/2}\tau^{1/2}\frac{d\bar{P}}{dx} - \frac{Gr_{D_h}}{Re_{D_h}^{3/2}}\tau^{1/2}\bar{T}_i - \frac{Gr_{D_h}(1-\bar{T}_i)\tau^{1/2}}{Re_{D_h}^{3/2}}\frac{Pr^{1/2}-1}{Pr-1}. \quad (10)$$

Noting that $Pr-1 = (Pr^{1/2}-1)(Pr^{1/2}+1)$, solving equation (10) for $1/\tau^{1/2}$, and substituting the result into equation (8) produces

$$Nu_{D_h} = 0.5\sigma_0\, Pr^{1/2}\left(\frac{1-\bar{T}_i}{\bar{u}_i}\right)\left[1+\sqrt{\left(1+\frac{4Re_{D_h}^{1/2}\bar{u}_i}{\sigma_0^2}\times\left[Re_{D_h}^{1/2}\frac{d\bar{P}}{dx}+\frac{Gr_{D_h}}{Re_{D_h}^{3/2}(Pr^{1/2}+1)}(1+Pr^{1/2}\bar{T}_i)\right]\right)}\right]. \quad (11)$$

In this equation $\bar{T}_i$ and $\bar{u}_i$ represent the initial temperature and velocity, respectively, of a clump of fluid impinging on the wall. These quantities are assumed to be equal to the free stream values of $\bar{T}_i = 0$ and $\bar{u}_i = 1$. It should be noted however that the assumption $u_i = 1$ breaks down for high Pr since the inrushing clump of fluid seldom moves into the direct contact with the wall [15], thereby attenuating u_i. The pressure gradient and the wall shear stress can be defined in terms of a forced convection friction factor given as

$$\frac{d\bar{P}}{dx} = -\frac{f}{2}$$

and

$$\sigma_0 = Re_{D_h}\frac{f}{8}.$$

Substituting these expressions and the assumed initial conditions into equation (11) produces

$$Nu_{D_h} = 0.0625 f Re_{D_h} Pr^{1/2}\left[1+\sqrt{\left(1-\frac{128}{Re_{D_h} f}+256\frac{Gr_{D_h}}{Re_{D_h}^3(Pr^{1/2}+1)}\frac{1}{f^2}\right)}\right]. \quad (12)$$

From forced convection data (Kays and Crawford [19])

$$f = 4C_f = 0.184 Re_{D_h}^{-0.2}.$$

Substituting this expression into equation (12) gives

$$Nu_{D_h} = 0.0115 Re_{D_h}^{0.8} Pr^{0.5}\left[1+\sqrt{\left(1-\frac{696}{Re_{D_h}^{0.8}}+7561\frac{Gr_{D_h}}{Re_{D_h}^{2.6}(Pr^{0.5}+1)}\right)}\right]. \quad (13)$$

RESULTS AND DISCUSSION

Equation (13) shows the variation in the forced convection Nusselt number with the pressure gradient and with an opposing buoyancy effect. Note that this equation reduces to the Dittus–Boelter correlation when the pressure and buoyancy terms are neglected. The positive sign in front of the buoyancy term accounts for the enhanced heat transfer associated with opposing mixed turbulent flows.

It is interesting to compare the buoyancy term in equation (13) and the one in Jackson and Fewster's correlation (equation (1)). The primary difference lies in the Prandtl number dependence in the denominator. The theory derived in this work contains $Pr^{1/2}+1$ in the denominator while the Jackson and Fewster correlation contains $Pr^{1/2}$ in the denominator. Jackson and Fewster's correlation underpredicts both Axcell and Hall's data [6] for air and the data of Swanson and Catton [20] for Freon 113 by about 30% implying that the Prandtl number dependence in the correlation may not be correct.

Figure 2 shows a comparison of equation (13) with data for air, Freon 113, and Jackson and Fewster's correlation for water ($Pr = 2.25$). The average density in Jackson and Fewster's correlation was approximated by substituting the Boussinesq approximation for the local density in equation (3). The bulk temperature (T_b) was assumed to be equal to the free stream temperature since velocity and temperature distributions were not explicitly given. Equation (13), based solely on a forced convection friction factor, agrees with the data for $Gr_{D_h}/Re_{D_h}^{2.6}(Pr^{0.5}+1) < 5\times10^{-4}$. Above this point, the forced flow friction factor law breaks down due to the buoyancy effect in the wall layer. The data indicate that the mixed friction factor is less than the forced friction factor for the same Reynolds number. This deviation can be accounted for in equation (13) by adjusting both the coefficient multiplying the mixed convection

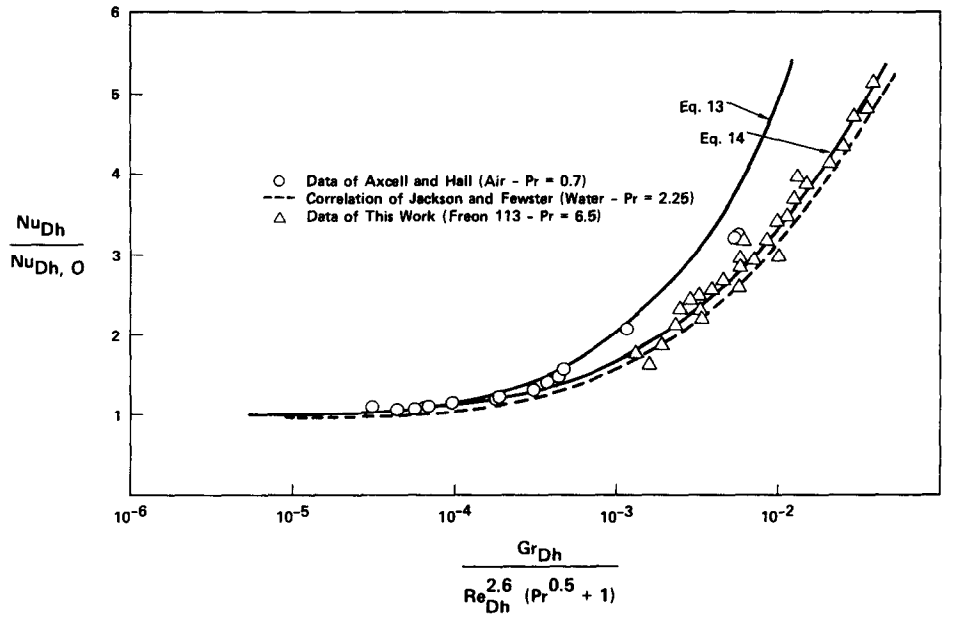

FIG. 2. Comparison of theory to data for various Prandtl number fluids.

dimensionless group and the power law dependence. The resulting correlation is given by

$$Nu_{D_h} = 0.0115 Re_{D_h}^{0.8} Pr^{0.5} \left\{1 + \left[1 - \frac{696}{Re_{D_h}^{0.8}} + 8300 \frac{Gr_{D_h}}{Re_{D_h}^{3}(Pr^{0.5}+1)}\right]^{0.39}\right\} \quad (14)$$

with less than a 7% r.m.s. error, which is well within the experimental error of 12%. This function is shown to fit the data for air, water and Freon 113 very well in Fig. 2. The mean wall residence time can now be evaluated by solving for τ with $\bar{T}_i = 0$ in equation (8) giving

$$\tau = \frac{Re_{D_h} Pr}{Nu_{D_h}^2}. \quad (15)$$

Substituting equation (14) for Nu_{D_h} in equation (15) produces

$$\tau = \frac{7561 Re_{D_h}^{-0.6}}{\left[1 + \left(1 - \frac{696}{Re_{D_h}^{0.8}} + 8300 \frac{Gr_{D_h}}{Re_{D_h}^{2.6}(Pr^{0.5}+1)}\right)^{0.39}\right]^2}. \quad (16)$$

This expression for the dimensionless mean wall residence time distribution is plotted in Fig. 3 as a function of the mixed flow dimensionless group with the Reynolds number as a parameter. The figure shows that the mean wall residence time distribution decreases as both $Gr_{D_h}/Re_{D_h}^{2.6}(Pr^{0.5}+1)$ and Re_{D_h} increase. This behavior is due to the enhanced mixing caused by either the increased opposing buoyancy force or the increased viscous shearing force. The heat transfer also increases since the fluid is being exchanged more frequently on the wall.

Now that τ is known, the velocity profile can be evaluated after setting $\bar{T}_i = 0$ and $\bar{u}_i = 1$ in equation (9). Utilizing the forced friction factor relationship for $d\bar{P}/dx$ produces

$$\bar{u} = \left(1 + \frac{0.092}{Re_{D_h}^{0.2}}\tau\right)(1 - e^{-ay}) - \frac{Gr_{D_h}\tau}{(Pr-1)Re_{D_h}^2}(e^{-ay} - e^{-by}) \quad (17)$$

where τ is evaluated from equation (16). It should be noted that a singularity occurs in this expression for $Pr = 1$. Applying l'Hopital's rule to the buoyancy term for $Pr = 1$ yields

$$\bar{u} = \left(1 + \tau \frac{0.092}{Re_{D_h}^{0.2}}\right)(1 - e^{-ay}) - \frac{Gr_{D_h}\tau^{0.5}}{2Re_{D_h}^{1.5}} y e^{-ay}. \quad (18)$$

The expression for the temperature profile is determined by setting $\bar{T}_i = 0$ in equation (6) and noting that $Nu_{D_h} = b$ in equation (8). The temperature distribution simply becomes

$$\bar{T} = e^{-Nu_{D_h} y}. \quad (19)$$

It should be noted that equations (17)–(19) are valid only near the wall and become less dependable as the free stream is approached. Equations (17) and (19) are plotted to demonstrate the parametric trends associated with the near wall flow field.

Figure 4 shows the variation of the velocity profile with the Reynolds number for constant Grashof and Prandtl numbers. The velocity and temperature profiles are not expressed in terms of the inner spacial

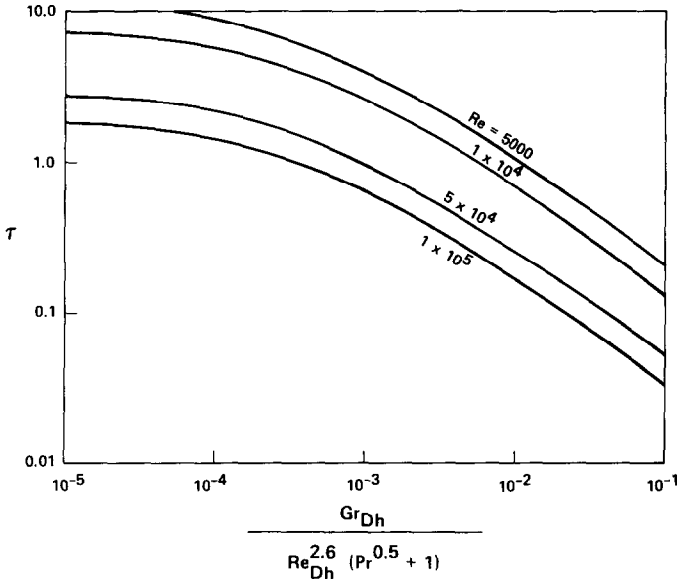

FIG. 3. Mean wall residence time as a function of the mixed dimensionless group with the Reynolds number as a parameter.

variable (y^+) since it is possible that the value of the shear at the wall is equal to zero. As expected, the effect of the buoyancy force near the wall increases as the Reynolds number is decreased. This effect manifests itself by decreasing the velocity near the wall. For this set of parameters, the buoyancy effect becomes so strong that a mean velocity flow reversal occurs in the neighborhood of $Re_{D_h} = 1 \times 10^4$. At this point, the fluid flows upward near the wall in the negative direction. These flows tend to steepen the velocity profile near the edge of the boundary layer causing the enhanced mixing alluded to earlier. As the Reynolds number continues to decrease, the minimum value of the velocity moves outward away from the wall. Figure 4 also shows that the momentum boundary layer thickness increases with decreasing Reynolds number.

Figure 5 shows the temperature profile for various Reynolds numbers with the Grashof number and Prandtl number constant. The figure shows that the thermal boundary layer, in general, decreases with increasing Reynolds number. However, for this particular set of parameters, Reynolds numbers of 5×10^3 and 1×10^4 produce the same temperature profile. In this case, the Nusselt number given by equation (14) remains constant because the decrease in Reynolds number increases $Gr_{D_h}/Re_{D_h}^{2.6}(Pr^{0.5}+1)$ enough to balance the decrease in $Re_{D_h}^{0.8}$ outside the brackets. This phenomena arises because the degree of fluid mixing which determines the heat transport is dependent on both the buoyancy force and the viscous shearing force. The relative increase in buoyancy at $Re_{D_h} = 5 \times 10^3$ produces the same amount of mixing as the relative increase in viscous shearing at $Re_{D_h} = 1 \times 10^4$.

Figure 6 shows the velocity profile for constant Reynolds and Prandtl numbers with the Grashof

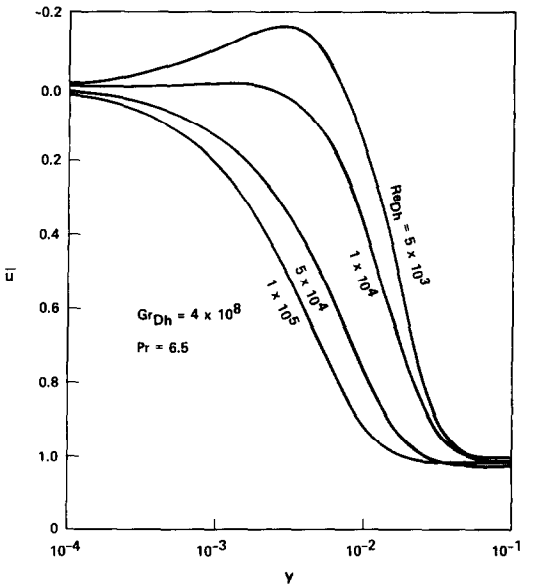

FIG. 4. Variation of the velocity profile with the Reynolds number for constant Grashof and Prandtl numbers.

number as a parameter. The profiles indicate that the momentum boundary layer thickness decreases as the Grashof number increases. This seems somewhat contrary to intuition since one would expect the additional shearing due to the downward flowing free stream to thicken an upward flowing buoyant layer. However, experimental observations (see Swanson [21]) indicate that the buoyant layer is actually sheared off near the upper leading heated edge inducing rapid momentum boundary layer development on the order of one hydraulic diameter in length. The buoyant layer thickness remains constant beyond this point. These observations suggest that the increased shearing actu-

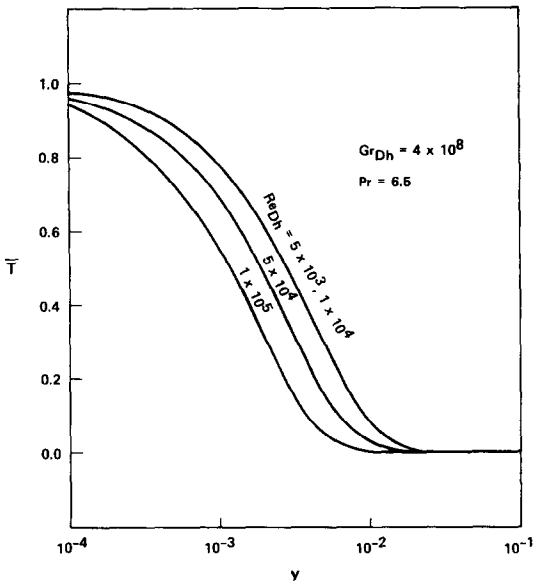

FIG. 5. Temperature profiles for various Reynolds numbers for a constant Grashof number and Prandtl number.

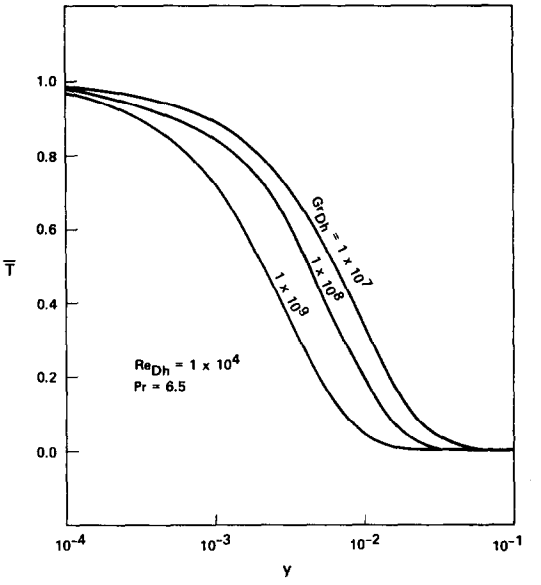

FIG. 7. Temperature profiles for constant Reynolds and Prandtl numbers with the Grashof number as a parameter.

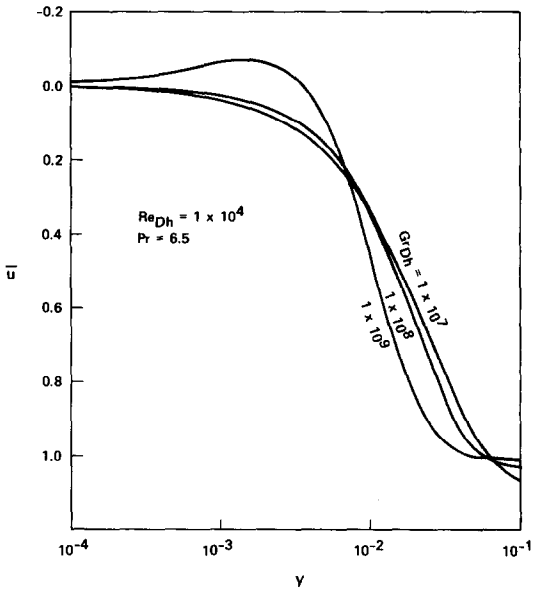

FIG. 6. Velocity profiles for constant Reynolds and Prandtl numbers with the Grashof number as a parameter.

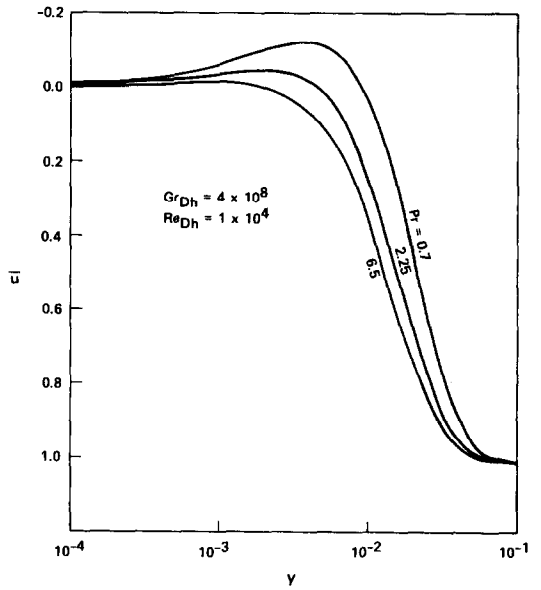

FIG. 8. Velocity profiles for constant Reynolds and Grashof numbers with the Prandtl number as a parameter.

ally reduces the momentum boundary layer thickness and increases mixing within the layer. Figure 7 shows that the increased mixing due to buoyancy manifests itself in reducing the thermal boundary layer thickness, thus enhancing heat transfer.

Figure 8 shows the effect of the Prandtl number on the velocity profile. As the Prandtl number decreases, the buoyancy effect increases and the minimum point in the mean velocity moves outward toward the free stream. This is expected since the buoyancy term in equation (18) is inversely proportional to $(Pr-1)$. It is interesting to note that the momentum boundary layer thickness remains relatively constant as the Prandtl number is varied. Figure 9 shows that decreasing the Prandtl number increases the thermal boundary layer thickness. As the thermal boundary layer thickens, warmer fluid extends further outward toward the free stream which produces the thicker upward flowing buoyant layer shown in Fig. 8.

CONCLUSIONS

A study of opposing mixed turbulent convection in vertical ducts was conducted utilizing surface renewal theory. The heat transfer correlation was found to be

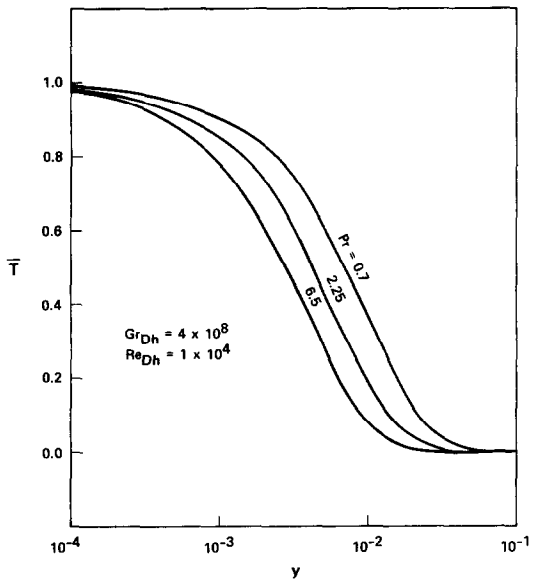

FIG. 9. Temperature profile for constant Reynolds and Grashof numbers with the Prandtl number as a parameter.

$$Nu_{D_h} = 0.0115 Re_{D_h}^{0.8} Pr^{0.5} \left\{1 + \left[1 - \frac{696}{Re_{D_h}^{0.8}} + 8300 \frac{Gr_{D_h}}{Re_{D_h}^{2.6}(Pr^{0.5}+1)}\right]^{0.39}\right\}.$$

The correlation fit the data to within 7% over a parameter range of $0.7 < Pr < 7$, $1 \times 10^4 < Re_{D_h} < 2 \times 10^4$ and $1 \times 10^6 < Gr_{D_h} < 2 \times 10^9$. The surface renewal mechanism provided valuable insight into the physics of turbulent flow phenomena in the wall layer. The mean residence time, characterizing the time a clump of fluid resides on the wall, was found to decrease as both $Gr_{D_h}/Re_{D_h}^{2.6}(Pr^{0.5}+1)$ and Re_{D_h} increase. This explains the enhanced heat transfer due to buoyancy in opposing mixed turbulent flows. This heat transfer enhancement was also reflected in a decreasing thermal boundary layer thickness with increasing Re_{D_h}, Gr_{D_h} or Pr.

Acknowledgement—The authors gratefully acknowledge the support of the Electrical Power Research Institute under Project RP2122-9.

REFERENCES

1. M. Nakajima, K. Fukui, H. Ueda and T. Mizushina, Buoyancy effects on turbulent transport in combined free and forced convection between parallel plates, *Int. J. Heat Mass Transfer* **23,** 1325–1336 (1980).
2. T. Cebeci, A model for eddy conductivity and turbulent Prandtl number, *J. Heat Transfer* **92C,** 227–234 (1973).
3. M. R. Doshi and W. N. Gill, A note on the mixing length theory of turbulent flow, *A.I.Ch.E. Jl* **16**(5), 885–888 (1970).
4. P. H. Oosthuizen, Turbulent combined convective flow over a vertical plane surface, Fifth IHTC, Tokyo, Japan, Vol. 3, No. 4.1, pp. 129–133 (1974).
5. J. D. Jackson and J. Fewster, Enhancement of heat transfer due to buoyancy for downward flow of water in vertical tubes, ICHMT, International Seminar on Turbulent Buoyant Convection, Dubrovnik, Yugoslavia, pp. 759–775 (1977).
6. B. P. Axcell and W. B. Hall, Mixed convection to air in a vertical pipe, Sixth IHTC, Toronto, Canada, MC-7, pp. 37–42 (1978).
7. J. D. Jackson, Turbulent mixed convection heat transfer to liquid sodium, *J. Heat Fluid Flow* **4**(2), 107–111 (1983).
8. B. S. Petukhov and V. V. Kirillov, The problem of heat exchange in the turbulent flow of fluids in tubes, *Teploenegetika* **4,** 63–68 (1958).
9. A. Watzinger and D. G. Johnson, *Forschung-Ing. Wesen* **10,** 182–196 (1939).
10. L. S. Herbert and U. J. Sterns, Heat transfer in vertical tubes—interaction of forced and free convection, *Chem. Engng J.* **4,** 46–52 (1972).
11. L. C. Thomas, Temperature profiles for liquid metals and moderate-Prandtl-number fluid, *J. Heat Transfer* **92,** 565–567 (1970).
12. L. C. Thomas and L. T. Fan, A model for turbulent transfer in the wall region, *ASCE J. Engng Mech. Div.* **97,** 169 (1971).
13. L. C. Thomas, B. T. F. Chung and S. K. Mahaldar, Temperature profiles for turbulent flow of high Prandtl number fluids, *Int. J. Heat Mass Transfer* **14,** 1665 (1971).
14. L. C. Thomas and M. L. Wood, A new approach to the analysis of turbulent free convection heat transfer, *Int. J. Heat Fluid Flow* **1**(2), 93–96 (1979).
15. L. C. Thomas and C. R. Kakarala, A unified model for turbulent and laminar momentum transfer: channel flow, *Trans. Am. Soc. Mech. Engrs* 8–12 (1976).
16. R. Higbie, The rate of absorption of a pure gas into a still liquid during short periods of exposure, *A.I.Ch.E. Trans.* **31,** 365–389 (1935).
17. R. V. Danckwerts, Significance of liquid-film coefficients in gas adsorption, *Ind. Engng Chem.* **43,** 1460–1467 (1951).
18. H. A. Einstein and H. Li, The viscous sublayer along a smooth boundary, *ASCE Engng Mech. Div. J.* **82** (No. E. M.), 1–17 (1956).
19. W. M. Kays and M. E. Crawford, *Convective Heat and Mass Transfer*. McGraw-Hill, New York (1980).
20. L. W. Swanson and I. Catton, Enhanced heat transfer due to secondary flows in mixed turbulent convection, *J. Heat Transfer* (1987), in press.
21. L. W. Swanson, Mixed turbulent convective heat transfer in ducts, Ph.D. Dissertation, University of California, Los Angeles (1987).

THEORIE DU RENOUVELLEMENT DE SURFACE POUR LA CONVECTION TURBULENTE MIXTE DANS DES TUBES VERTICAUX

Résumé—Une formule de transfert thermique pour la convection turbulente mixte avec opposition, dans des tubes verticaux, est obtenue à partir d'une théorie de renouvellement de surface:

$$Nu_{D_h} = 0{,}0115 Re_{D_h}^{0,8} Pr^{0,5}\left\{1+\left[1-\frac{696}{Re_{D_h}^{0,8}}+8300\frac{Gr_{D_h}}{Re_{D_h}^{2,6}(Pr^{0,5}+1)}\right]^{0,39}\right\}.$$

La formule représente les données à 7% près pour un domaine $0{,}7 < Pr < 7$; $1.10^4 < Re_{D_h} < 2.10^4$ et $1.10^6 < Gr_{D_h} < 2.10^9$. Le temps de séjour, caracterisant le temps de résidence d'une particule fluide sur la paroi, décroît aussi bien lorsque $Gr_{D_h}/Re_{D_h}^{2,6}(Pr^{0,5}+1)$ et Re_{D_h} augmentent. Ceci explique l'amélioration du transfert thermique due au flottement dans les écoulements turbulents mixtes avec opposition. L'accroissement de transfert est aussi reflété par la diminution de l'épaisseur de la couche limite thermique quand augmentent Re_{D_h}, Gr_{D_h} ou Pr.

OBERFLÄCHEN-ERNEUERUNGS-THEORIE BEI DER TURBULENTEN MISCH-KONVEKTION IN SENKRECHTEN KANÄLEN

Zusammenfassung—Unter Anwendung der Oberflächen-Erneuerungs-Theorie wurde eine Wärmeübergangs-Korrelation für die gegengerichtete turbulente Misch-Konvektion in senkrechten Kanälen gefunden:

$$Nu_{D_h} = 0{,}0115\, Re_{D_h}^{0,8}\, Pr^{0,5}\left\{1+\left[1-\frac{696}{Re_{D_h}^{0,8}}+8300\frac{Gr_{D_h}}{Re_{D_h}^{2,6}(Pr^{0,5}+1)}\right]^{0,39}\right\}.$$

Die Korrelation zeigt eine maximale Abweichung von sieben Prozent für folgende Parameter-Bereiche: $0{,}7 < Pr < 7$, $1\ 10^4 < Re_{D_h} < 2\ 10^4$ und $1\ 10^6 < Gr_{D_h} < 2\ 10^9$. Die mittlere Aufenthaltsdauer eines Fluidteilchens an der Behälterwand, nimmt mit wachsenden Werten von $Gr_{D_h}/Re_{D_h}^{2,6}(Pr^{0,5}+1)$ und Re_{D_h} ab. Dies erklärt die Tatsache, daß der Wärmeübergang bei gegengerichteter turbulenter Misch-Konvektion durch Auftrieb verbessert wird. Die Verbesserung der Wärmeübertragung wird auch durch die abnehmende Grenzschichtdicke mit zunehmenden Werten von Re_{D_h}, Gr_{D_h} oder Pr bestätigt.

ТЕОРИЯ ОБНОВЛЕНИЯ ПОВЕРХНОСТИ ПРИМЕНИТЕЛЬНО К ТУРБУЛЕНТНОЙ СМЕШАННОЙ КОНВЕКЦИИ В ВЕРТИКАЛЬНЫХ КАНАЛАХ

Аннотация—С помощью теории обновления поверхности получено полуэмпирическое соотношение для теплообмена в случае противоположно направленной смешанной турбулентной конвекции в вертикальных каналах. Соотношение имеет вид

$$Nu_{D_h} = 0{,}0115 Re_{D_h}^{0,8}\ Pr^{0,5}\left\{1+\left[1-\frac{696}{Re_{D_h}^{0,8}}+8300\frac{Gr_{D_h}}{Re_{D_h}^{2,6}(Pr^{0,5}+1)}\right]^{0,39}\right\}.$$

Оно согласуется с экспериментальными данными с точностью до 7% в следующих диапазонах изменения параметров: $0{,}7 < Pr < 7$, $1 \times 10^4 < Re_{D_h} < 2 \times 10^4$ и $1 \times 10^6 < Gr_{D_h} < 2 \times 10^9$. Найдено, что среднее время обновления, характеризующее время контакта жидкости, вносимой из внешней области, со стенкой, уменьшается с увеличением $Gr_{D_h}/Re_{D_h}^{2,6}(Pr^{0,5}+1)$ и Re_{D_h}. Это обстоятельство объясняет увеличение интенсивности теплообмена за счет естественной конвекции в противоположно направленных турбулентных потоках при смещанной конвекции. Такое увеличение теплообмена согласуется с уменьшением толщины теплового пограничного слоя при возрастании Re_{D_h}, Gr_{D_h} и Pr.